Please cite this paper as:

Wang, Z., Pan, W., & Zhang, Z. (2020). High-rise modular buildings with innovative precast concrete shear walls as a lateral force resisting system, *Structures*, *26*: 39-53. doi: 10.1016/j.istruc.2020.04.006

High-rise modular buildings with innovative precast concrete shear walls as a lateral force resisting system

Zhen Wang, Wei Pan*, and Zhiqian Zhang

Department of Civil Engineering, The University of Hong Kong, Pokfulam, Hong Kong, China

Abstract: Modular construction has been widely adopted for low-to-medium-rise buildings, but fairly limited for high-rises. A particular knowledge gap resides with the lateral force resistance of modular high-rises. Most such buildings adopt cast-in-situ cores for lateral force resisting, which is still labor-intensive. This paper aims to develop a new lateral force resisting system using precast shear walls as part of the modules for high-rises. A 40-story public housing building in Hong Kong was used for case study. A finite element (FE) model was developed to simulate the structural performance of the precast concrete shear walls and validated using results of cyclic loading tests. Using the FE model nonlinear static and dynamic analyses were conducted to examine the feasibility of the proposed system under the wind and seismic loadings in relevant codes. Multi-modal analysis further investigates the effects of higher modes on the seismic responses of the building. Results show that the developed FE model is effective to reproduce the structural performance of the precast concrete shear walls, and the proposed system is strong enough to resist wind and seismic loadings. Higher modes have considerable even dominant effects on seismic responses of the building. Using the cumulative contribution of modes to seismic demands is found appropriate to help select modes to calculate the seismic demands of high-rise modular buildings with the proposed lateral force resisting system.

*Corresponding author. *E-mail address*: wpan@hku.hk

Keywords: high-rise building; modular integrated construction; precast concrete; lateral force resisting system; nonlinear dynamic analysis; higher modes

1. Introduction

Modular construction has been widely used in many countries and regions including US, UK, Germany, Canada, Australia, Singapore and China [1-3]. The modular approach has wide-ranging demonstrated benefits of shortened onsite construction time, reduced resource waste, and enhanced quality, compared with conventional cast-in-situ construction methods [4-7].

High-rise buildings become more attractive than low-to-medium-rise buildings in metropolises with limited developable land resources. Although modular construction has been widely utilized for low-to-medium-rise buildings, it is limited for high-rise buildings [8]. One of the reasons is the lack of knowledge about the lateral force resistance of high-rise buildings if constructed using the modular approach. Lateral loadings on high-rises mainly refer to wind and seismic loadings. On the one hand, wind loading generally becomes dominant with the increased building height from the structural engineering point-of-view. On the other hand, many cities have raised their seismic fortification levels to reduce potential loss of life and property during an earthquake. Meanwhile, higher modes than the foundational mode have non-negligible effects on the seismic responses of high-rise buildings, which is different from low-to-medium-rise buildings [9]. Therefore, it is necessary to examine the lateral force resistance when planning and designing a high-rise building with the intention of adopting modular construction.

Some researchers examined lateral force resistance of modular buildings. Annan et al. [10-11] conducted experimental research on the cyclic performance of a modular steel building (MSB) braced frame compared with a traditional concentrically braced frame. They also conducted incremental dynamic analysis (IDA) on 2-, 4- and 6-story buildings with MSB braced frames, respectively. For a 10-story modular building, nonlinear static analysis was conducted to study its wind responses while nonlinear dynamic analysis was conducted to investigate its seismic responses according to the American codes [12-13]. Gunawardena et al. [14] put forward an innovative lateral force resisting system using bolted plate connections and added stiff concrete walls of steel modules to resist lateral loadings for a 20-story modular building. Styles et al. [15] selected an 11-story modular building as an objective to study the effect of joint rotational stiffness on wind responses. Fathieh and Mercan [16] conducted nonlinear static analysis and IDA on a 4-story building with

MSB braced frames. Srisangeerthanan et al. [17] studied the effects of in-plane diaphragm stiffness and strength on the seismic behavior of multi-story modular buildings. Shan et al. [18] preliminarily explored the feasibility of engineering modular integrated construction (MiC) using ETABS model for 31-story and 40-story high-rise buildings in Hong Kong (HK) where wind loading is a major consideration for structural design.

Despite the increasing research into lateral force resistance of modular buildings, there are still research gaps. First, very few previous studies examined lateral force resistance of modular buildings with over 20 stories. Second, little research focused on lateral force resistance of concrete modular buildings. Third, no special research investigated the contributions of higher modes on seismic responses of modular buildings.

Most medium-to-high-rise modular buildings adopted cast-in-situ concrete or steel cores to withstand the entire lateral loadings, which still need a mass of onsite concrete construction. Developing a novel lateral force resisting system requiring no core structures except modules walls for high-rise modular buildings has been found to be potentially useful but scientifically challenging. Hence, this paper aims to develop a novel lateral force resisting system using precast concrete shear walls for high-rise modular buildings. Those precast concrete shear walls are part of concrete modules and no additional structure is required. To achieve the aim, three research objectives are developed: (1) to propose the novel lateral force resisting system; (2) to check the feasibility of the proposed system under wind and seismic loadings; and (3) to investigate the effects of higher modes on seismic responses of high-rise modular buildings with the proposed system. The structure of the paper is as follows. First, a 40-story high-rise building using public housing design in HK is proposed as the case to characterize the proposed lateral force resisting system. Second, a finite element (FE) model of the precast concrete shear wall is developed and validated using the results from the cyclic loading tests reported in the literature. Third, nonlinear dynamic and static analyses are conducted using the FE model to assess the feasibility of the proposed system under the wind and seismic loadings defined in the HK codes. Finally, the effects of higher-modes on the seismic responses of the case building are discussed before conclusions are drawn.

2. The proposed lateral force resisting system for the case building

HK is a metropolis with the largest number of high-rise buildings in the world due to its limited developable land supply and large population [19]. Meanwhile, HK faces some critical challenges such as shortage of labor and aging workforce in the construction industry. Therefore, the Chief Executive of the HK government in the 2017 and 2018 Policy Address promoted the application of modular integrated construction (MiC) for enhancing productivity and competitiveness [20].

In this research, a 40-story residential building was selected for case study, which has a regular rectangular plan and an innovative lateral force resisting system with the walls of the precast modules acting as shear walls. The case building has the total height of 110 m according to each story height of 2.75 m and the rectangular plane dimensions of 35 m × 14 m (Fig. 1). Each story has 14 "big" modules with the individual architectural function and one corridor, which belongs to a typical corridor arrangement of modules [21]. The two "big" modules at the center have lifts and staircases to undertake the transportation function of moving people and logistics as public zones; every other "big" module provides a private residential flat for a household; and the corridor connects the "big" resident and transportation modules. The width of precast modules should normally be no more than 2.5 m according to the transportation regulation in HK. Thus, a "big" module is divided into two precast modules in factory (Fig. 1). After the two precast modules are transported to the construction site, they are merged into one "big" module through the cast-in-site stripe connections (Fig. 2), which is built before or after hoisting according to the lifting capacity of tower crane. Xu et al. [22] proposed a cast-in-site stripe connection using the pre-embedded and in-situ bars as well as the in-situ stirrups for connecting precast modules, and testified that the proposed connection can integrate the two precast modules into one whole. In the following context, the modules will specifically refer to the "big" module to avoid ambiguity. With the outer dimensions of 5 m × 6 m x 2.75 m, each concrete module is made up of ceiling slab, floor slab, and four walls, and includes the precast part of semi-precast corridor slab and some protruding bars for horizontal and vertical connections (Fig. 2).

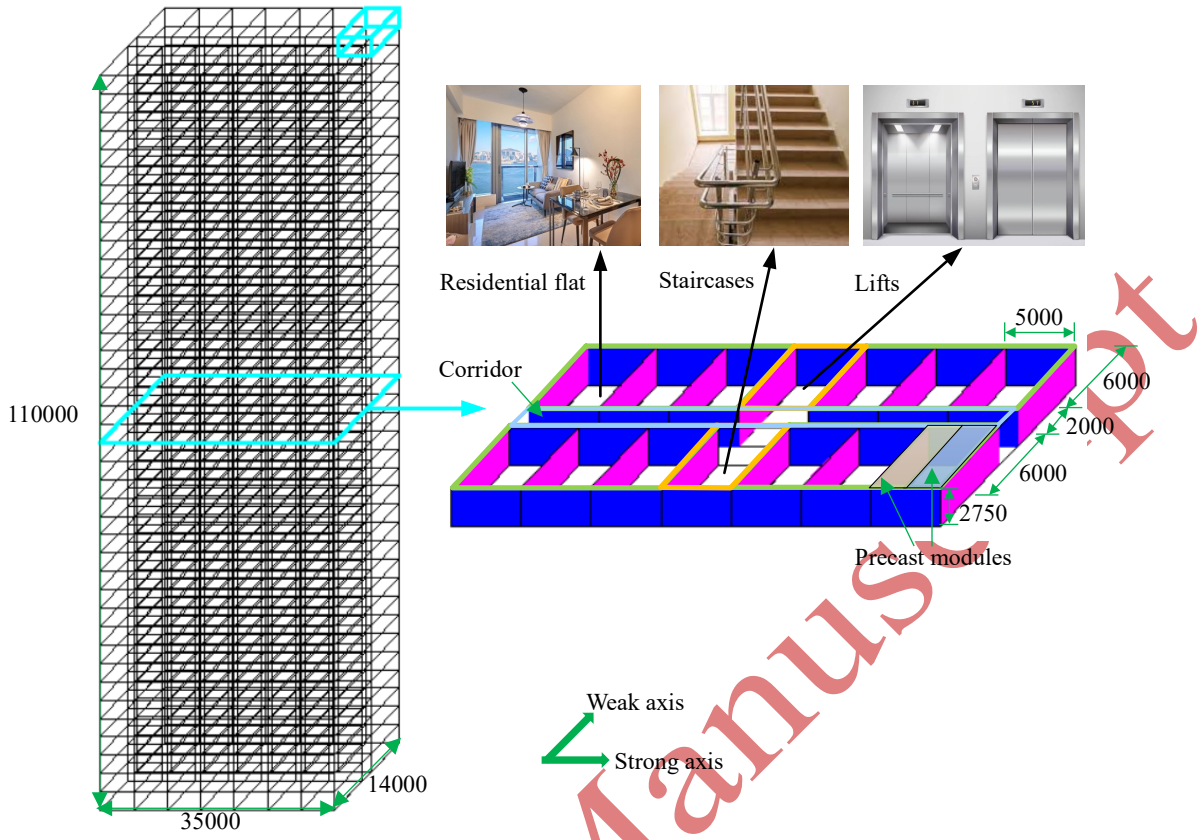

Fig. 1. Detailed information about the case building (unit: mm)

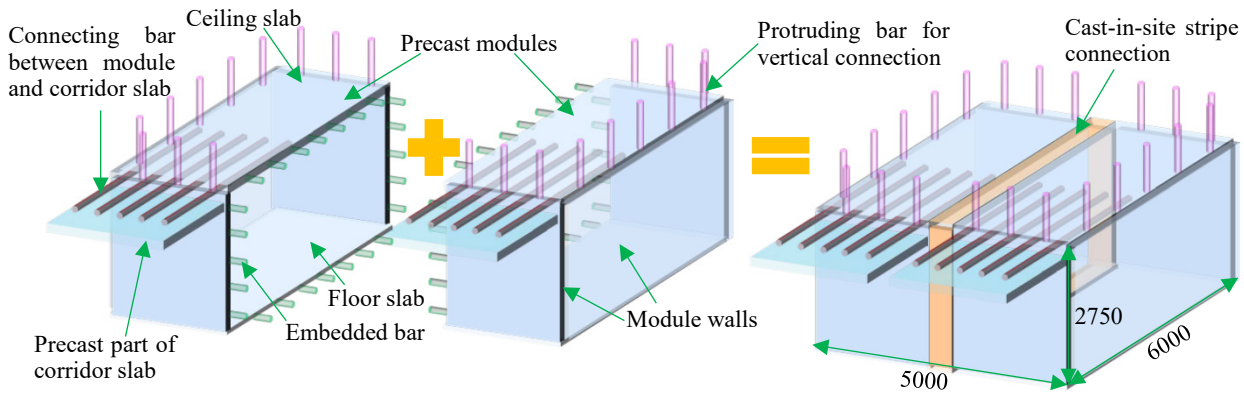

Fig. 2. Schematic diagram of a "big" module made up of two precast modules (unit: mm)

Uniform concrete modules are consumed to assemble the case building depending on various horizontal and vertical connections. The horizontal connections can be identified to two types: inter-module and module-to-corridor connections. Different from the bolted horizontal inter-steel module connections [6], the horizontal connections between the concrete modules adopt in-situ connecting bars and late cast concrete (Fig. 3) to integrate the ceiling slabs at one story into a whole

in the plane. Except the horizontal connection, no special construction details are used to connect the two adjacent walls of the different modules. The horizontal module-to-corridor connections are formed with the construction of semi-precast corridor slab, which is divided into two parts: the precast part connected with the modules (Fig. 2) can be used as the cast formwork for the cast-in-site part. The connecting bars between modules and the corridor slab (Fig. 2) are used to enhance the connection strength. All of the horizontal connections at the same story jointly work to ensure that the traditional rigid diaphragm assumption is still available for modular concrete structures. It is notable that there are no special construction details to connect the ceiling slab at one story and the floor slab at the above story. The rigid diaphragm effect of the modular building is designed to depend on the integrated ceiling slabs and semi-precast corridor slab at the same floor but does not consider the contribution of the floor slabs in the above level. The shear walls are formed using the structural walls of concrete modules, which are vertically connected using grouted sleeves. The rigid diaphragm effect can not only prevent lateral buckling of shear walls but also ensure all of the shear walls work together to resist lateral loading. Due to the regular plan, the torsion effect is not obvious and can be neglected for the case building. Meanwhile, the case building along the weak axis has the larger demand-to-capacity ratio to resist wind loading, which generally dominates the structural design of high-rise buildings in HK (Fig. 1). Thus, this study only focuses on the case building's lateral force resistance along the weak axis. It is notable that the two shear walls along the weak axis are deemed to work separately due to no special reinforcement constitution providing sufficient coupling effects for the two shear walls.

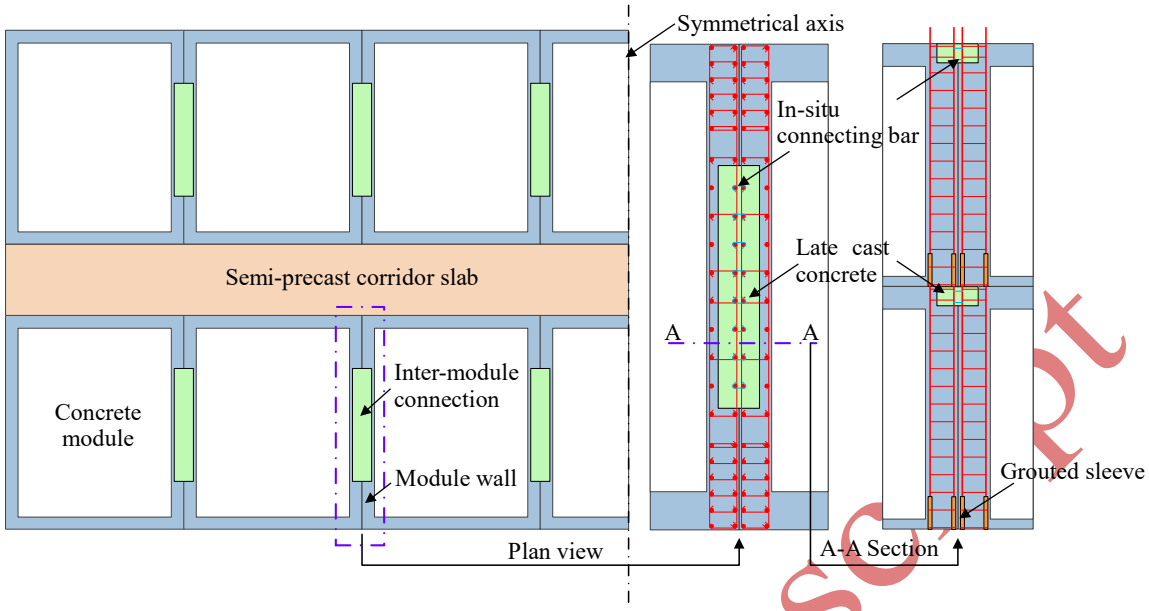

Fig. 3. The proposed horizontal and vertical connections in the case building

Each structural wall of concrete modules is designed to have the capacity of keeping the out-of-plane stability, bearing the axial loadings during the different phases of module handing, and resisting the lateral loadings such as wind loading, when the adopted construction details can enable that the rigid diaphragm assumption of the modular building is available and the vertical connection of walls using grouted sleeves is reliable. The structural wall of concrete modules is 2750 mm height and 200 mm thickness (Fig. 4). Its section is divided into two boundary elements with the height of 1000 mm and one web with the height of 4000 mm. Each boundary element uses twelve D20 bars as longitudinal bars and D10 bars with the vertical space of 100 mm as stirrups, while the web adopts twenty D20 bars as longitudinal bars and D10 bars with the vertical space of 200 mm as stirrups. Area ratios of the longitudinal bars are 1.88% and 0.79%, and the stirrup volume ratios are 1.80% and 0.65%, for the boundary element and the web, respectively. Double-row grouted sleeves are used to connect longitudinal bars between the two adjacent structural walls. The corresponding grouted sleeve to D20 bars has the outer diameter of 45 mm and the total length of 370 mm. The protruding bar of 165 mm is required to be inserted into the grouted sleeve [23].

The precast concrete modules are assumed to use C40 concrete and HRB400 reinforcement. C60 concrete is used as the grout material. The properties of those materials are provided in Table 1 and Table 2.

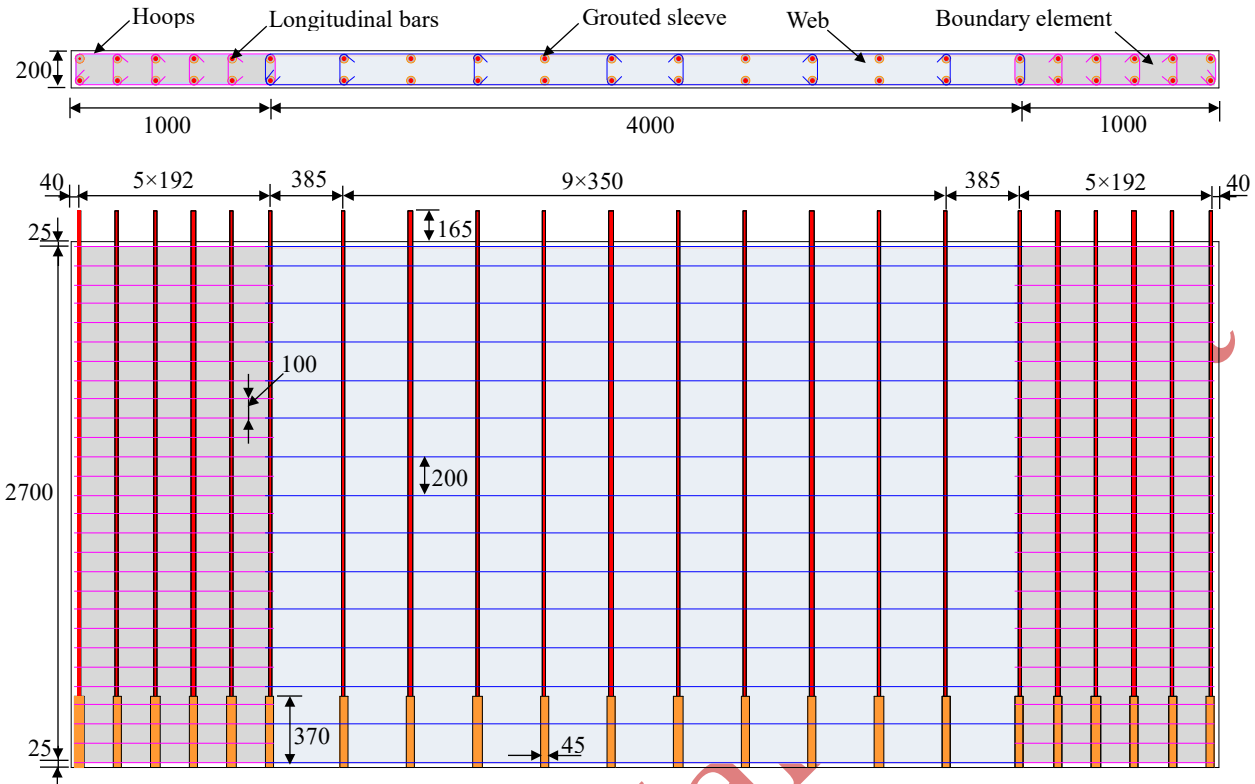

Fig. 4. Major design details of a structural wall of concrete modules (unit: mm)

Table 1 Material properties of deformed bars

Type	E_s/GPa	f_{sy}/MPa	ε_{sh}	E_{sh}/GPa	f_{su}/MPa	ε_{su}
D10	200	400	0.01	10	600	0.10
D20	200	400	0.01	10	600	0.10

Note: E_s is the elastic modulus of deformed bars; E_{sh} is the tangent at the initial strain hardening of deformed bars; f_{sy} and f_{su} are the yield and ultimate strengths of deformed bars, respectively; ε_{sh} and ε_{su} are the strains of deformed bars corresponding to the initial strain hardening and the ultimate strength, respectively.

Table 2 Material properties of concrete

Type	E_c/GPa	f_c/MPa	ε_{co}	f_t/MPa	v	ε_{cu}
C40	30.0	40	0.002	2.8	0.2	0.0038
C60	36.5	60	0.002	4.2	0.2	0.0038

Note: E_c is the elastic modular of concrete; f_c and f_t are the compressive and tensile strengths of concrete, respectively; v is the Poisson's ratio of concrete; ε_{co} and ε_{cu} are the strains of concrete corresponding to the compressive strength and the ultimate state, respectively.

3. Numerical modeling and experimental verification

3.1. Assumptions and simplifications

The 40-story case building can be built using the proposed modular construction method (Fig. 5). The precast concrete shear wall is deemed to have the identical structural performance to its cast-in-site counterpart, according to results of the cyclic loading tests on precast concrete shear

walls with grouted sleeve connections [24]. The equivalent dealing aims to focus on the overall structural responses of the case building under lateral loadings. As aforementioned, the rigid diaphragm assumption is deemed to be available for the case building in this research. Therefore, the lateral buckling of precast concrete shear walls is neglected in this model due to the lateral support of the ceilings at each story (Fig. 5), and all of the shear walls work together to resist the entire lateral loadings of the case building. It is notable that because the influence of the cumulative permanent drifts caused by the vertical inter-module connections can be effectively weakened by the rigid diaphragm, the influence is not specially considered for the case of concrete modules, which is different from the steel modular buildings. The vertical loadings $P_1 \sim P_{40}$ at the $1^{st} \sim 40^{th}$ stories result from the HK code specified live and dead loadings [25] in the bearing area of the objective shear wall, while the masses $m_1 \sim m_{40}$ at the $1^{st} \sim 40^{th}$ stories are determined using the combination of vertical loadings according to the code specifications [26]. As aforementioned, the two shear walls along the weak axis are deemed to work separately. Meantime, all of the shear walls have the identical lateral behavior due to their same structural design parameters and loading distributions, which are determined by structural characteristics of the modular building in this research. Thus, when the case building is subject to seismic or wind loading, all of the shear walls have the same structural responses. In other words, any slender shear wall can be selected to investigate the structural responses of the proposed novel lateral force resisting system in this research. Moreover, some other simplifications and assumptions in this research are given as follows: the shear walls are assumed to be fixed at the base; the selected ground motions are input from the base; and the Rayleigh damping model is available and the damping ratio is assumed to be 5% [27].

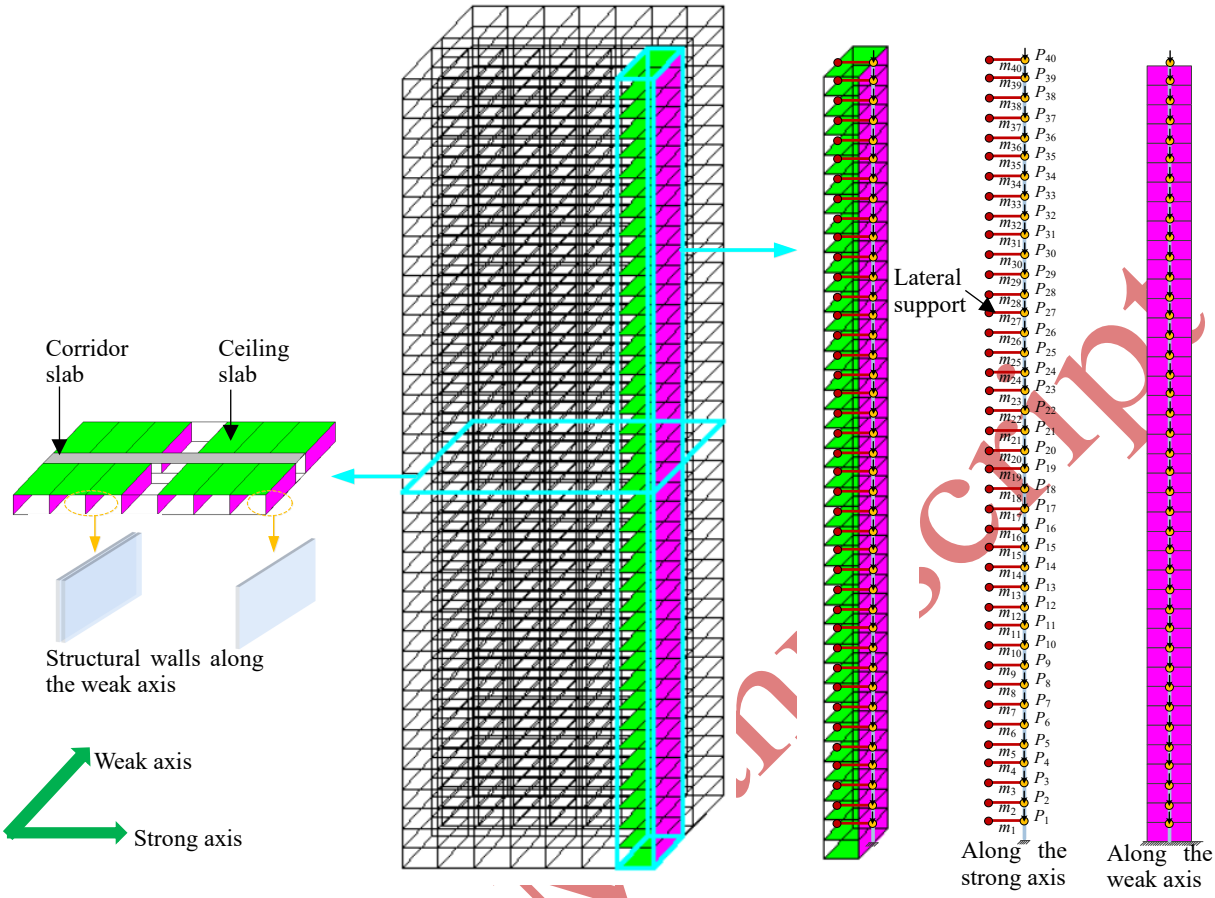

Fig. 5. Structural diagram of the case building built in the proposed modular construction method

3.2. Numerical modeling

Many numerical elements have been developed to simulate static and dynamic behaviors of concrete shear walls, such as simple macroscopic elements [28-30] and refined continuum elements [31]. The simple macroscopic elements include fiber beam-column element [28], multiple-vertical-line element [29], and multi-layer shell element [30]. Compared with other elements, fiber beam-column element has practical feasibility and efficiency, especially for nonlinear dynamic analysis, which generally requires plenty of computation time [32-34]. Many researchers suggested that the FE model using fiber beam-column element can successfully capture nonlinear static and dynamic responses of concrete shear walls [30]. Nonetheless, the simulated concrete shear walls must have the lateral deformation controlled by flexural behavior. When a concrete shear wall has the height-to-length ratio of greater than 3, its lateral deformation is generally dominated by flexural behavior. A FE model is developed using a range of tandem fiber beam-column elements to simulate the precast concrete shear wall (Fig. 6).

The axial-flexure behavior of the precast concrete shear wall is modeled through the fiber section in the developed FE model. The fiber section conforms to the assuming plane section and is composed of unconfined concrete fibers, confined concrete fibers, and bar fibers. The unconfined concrete fibers represent cover concrete and are defined by the Kent-Scott-Park model with linear tension softening, which is used to develop Concrete02 material model (Fig. 7(a)) in *OpenSees* platform [35]. The confined concrete fibers represent the core concrete in the boundary elements and the web. They can also be defined by Concrete02 material model. The confinement effect of stirrups on the core concrete can be determined according to the suggestion given by Kent and Park [36]. The bar fibers represent longitudinal bars and are defined by Reinforcing Steel material model (Fig. 7(b)) in *OpenSees* platform [35]. The material model can consider Bauschinger effect, low cycle fatigue behavior, buckling and so on [37].

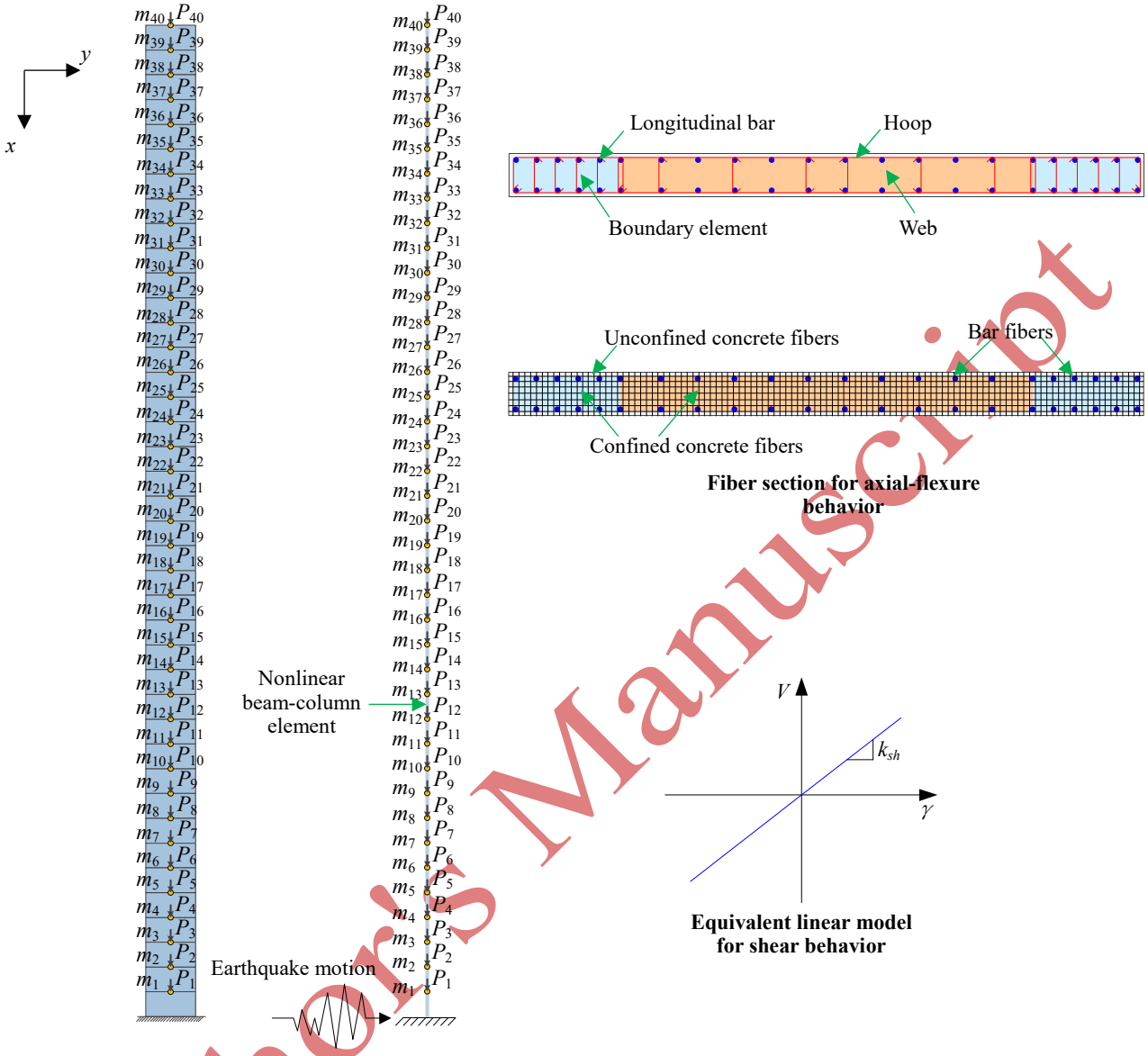

Fig. 6. The developed finite element model of the proposed precast concrete shear wall

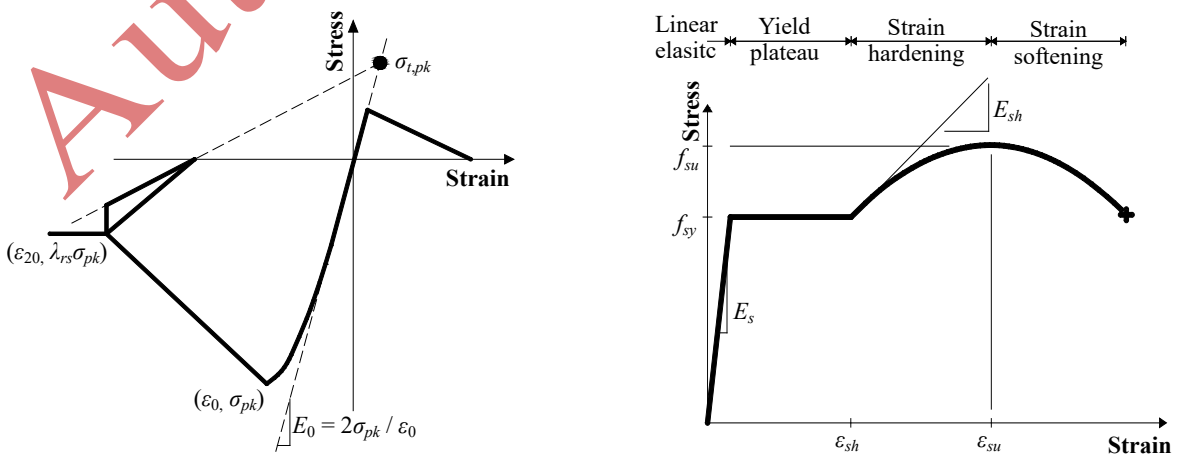

(a) Parameters of Concrete02 material model (b) Parameters of Reinforcing Steel material model

Fig. 7. Material models used in the developed finite element model

In the FE model, the shear behavior of the precast concrete shear wall is simplified to be equivalent linear behavior which is defined with the uncoupled shear sectional property. The equivalent shear stiffness k_{sh} is calculated with the reduced shear modulus of cracked concrete to indirectly consider the flexure-shear interaction as [28]

$$k_{sh} = \frac{5}{6} G_{cr} bh \tag{1}$$

where b and h are the sectional width and height, respectively. G_{cr} is the reduced shear modulus of cracked concrete and can be calculated as [37]

$$\frac{G_{cr}}{f_c} = 135\sqrt{\omega_x \omega_y} \tag{2}$$

where ω_x and ω_y are the reinforcement indexes in the x- and y- directions, respectively (Fig. 6). They can be calculated as

$$\omega_x = \frac{\rho_x f_{y-x}}{f_c} \le \kappa \tag{3}$$

$$\omega_y = \frac{\rho_y f_{y-y}}{f_c} \le \kappa \tag{4}$$

where ρ_x and ρ_y are the reinforcement ratios in the x- and y- directions, respectively. $f_{y\text{-}x}$ and $f_{y\text{-}y}$ are the yield strengths of reinforcement in the x- and y- directions, respectively. κ is the limit depending on the concrete compressive strength and given as

$$\kappa = \frac{1}{3} - \frac{f_c}{900} \tag{5}$$

3.3. Experimental verification

The developed FE model is verified by the experimental results of two shear wall specimens RW2 and PW1. Specimen RW2 is a one-quarter scale model specimen tested by Thomsen et al. [38]. After two cycles of 2.5% drift ratio, longitudinal bars in the compressive boundary element severely buckled, which can lead to significant loss of lateral force. Specimen PW1 is a one-third scale model specimen tested by Birely et al. [39]. Its failure was marked by the tensile fracture of longitudinal bars at the base. The two specimens have typical flexural failure modes. More detailed

information can be found in the references [38-39]. There is a good agreement between the predicted and experimental results of hysteretic curves (Fig. 8). Based on the previous research and conducted tests, the developed FE model in this paper is verified to be effective to simulate the cyclic behavior of concrete shear walls.

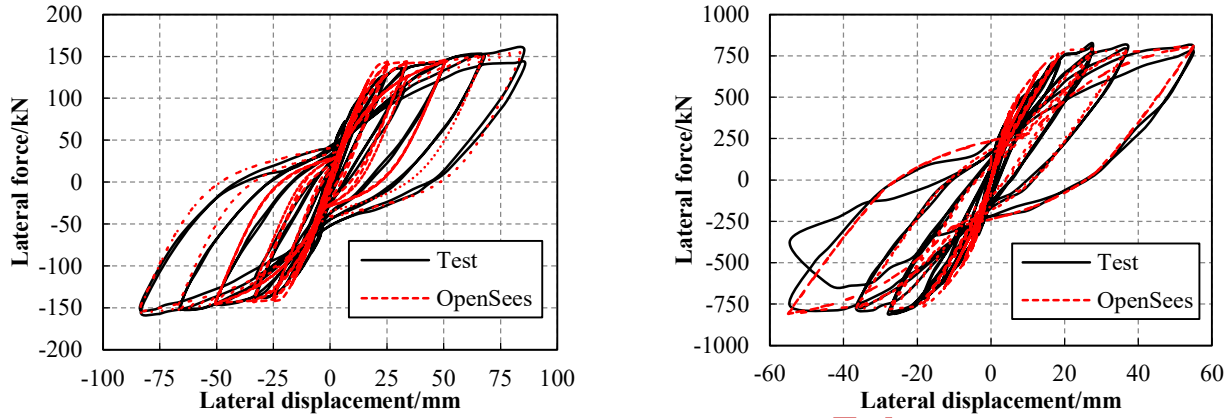

(a) Specimen RW2 (b) Specimen PW1

Fig. 8. Comparison of hysteretic curves between the experimental and simulated results

4. The proposed lateral force resisting system under wind loading

4.1. Calculation of wind loading considering the dynamic effect

Wind loading is a governing factor in the structural design of lateral force resistance for high-rise buildings in HK. The feasibility of the proposed lateral force resisting system is checked using the wind loading defined in the relevant code in HK [40]. When an enclosed building has the height of more than 100 m, the total along-wind force on the enclosed building must consider the dynamic effect according to the wind code of HK [40]. The calculation method of wind loading is detailed in Section 7 of the wind code of HK [40]. All the parameters can be determined according to the basic information of the case building except two parameters, which are the fundamental natural frequency f_1 of 0.175 Hz and the topography factor S_{tg} of 1.07 for the case building. The applied wind loading at each story is calculated for the single precast concrete shear wall along the weak axis of the case building (Fig. 9).

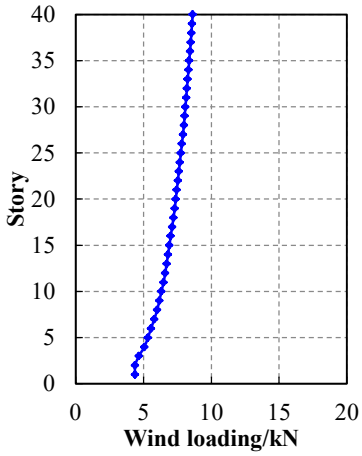

Fig. 9. Wind loading at each story for the precast concrete shear wall along the weak axis

4.2. Feasibility assessment

The wind loading was calculated for the precast concrete shear walls in the developed FE model. The wind responses including shear force, moment, and lateral deformation can be obtained as shown in Fig. 10. The maximum values of shear force and moment are at the bottom, which means that the bottom is most likely to be damaged. The capacities of resisting shear force and moment at the bottom are required for feasibility assessment.

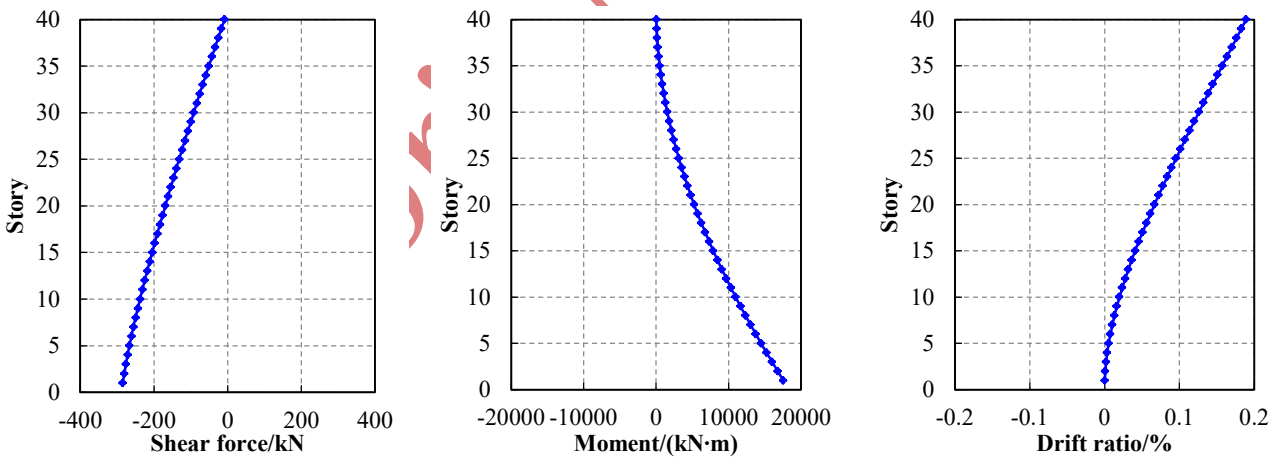

(a) Shear force (b) Moment (c) Lateral deformation

Fig. 10. Wind responses of the precast concrete shear wall

The design shear resistance of concrete members is regarded as the capacity of resisting shear force. The calculation method is detailed in the concrete code of HK [41]. The capacity of resisting shear force is 2870 kN at the bottom of the shear wall. The demand-capacity ratio of shear force is 0.099 at the bottom. These results indicate that the proposed lateral force resisting system has

enough capacity to resist the shear force caused by the wind loading defined in the code of HK.

The capacity of resisting moment is deemed to be the yield moment. Sectional analysis can calculate the yield moment using Zero-Length Section element which is defined with the identical fiber section to that used for the axial-flexure behavior (Fig. 6). The capacity of resisting moment is 28500 kN·m at the bottom of the shear wall. The demand-capacity ratio of moment is 0.616 at the bottom, which indicates that the proposed system has enough capacity to resist the moment caused by the wind loading defined in the code of HK.

The HK code stipulates that 0.2% is the upper limit of deflection at the top when a static characteristic wind loading is conducted on a building [41]. As shown in Fig. 10(c), the maximum drift ratio of 0.19% at the top is less than 0.2%, which indicates that the proposed system has enough stiffness to resist the lateral deformation caused by wind loading defined in the HK code.

It is noted that the above calculations of wind responses are preliminary for the case building with the fundamental natural frequency less than 0.2 Hz [40]. The dynamic wind tunnel model studies will be required in the future work to further check the feasibility of the proposed lateral force resisting system.

5. The proposed lateral force resisting system under seismic loading

5.1. Selection of ground motions

HK will soon raise seismic fortification grade from non-seismic to seismic fortification, with the draft seismic design code of HK [26] being finalized. The case building belongs to Importance Class C according to its ordinary residential usage [26]. Meantime, the construction site belongs to Ground Type B according to the surrounding borehole records [26]. The peak ground acceleration (PGA) of the design basis earthquake is 0.84g for a building of Importance Class C located in a construction site of Ground Type B [26]. Low, moderate, and high intensities of earthquake motions are suggested to be considered in HK. The probabilities of exceedance are 50%, 10% and 2% in 50 years, and the return periods are 72 years, 475 years and 2475 years, for the three intensities of earthquake motions, respectively [42]. The PGAs of the three intensities are 0.43, 1 and 2 times that of the design basis earthquake, respectively. Fig. 11 presents the target spectra for the three intensities of earthquake motions.

Seven earthquake motion records were selected from the NGA-West2 of PEER Ground Motion Database to match the target spectrum of the design basis earthquake. The selected earthquake motion records have the response spectra corresponding to 5% damping and the wave velocities conforming to the stipulations of Ground Type B. More information on the selected earthquake motion records is provided in Table 3.

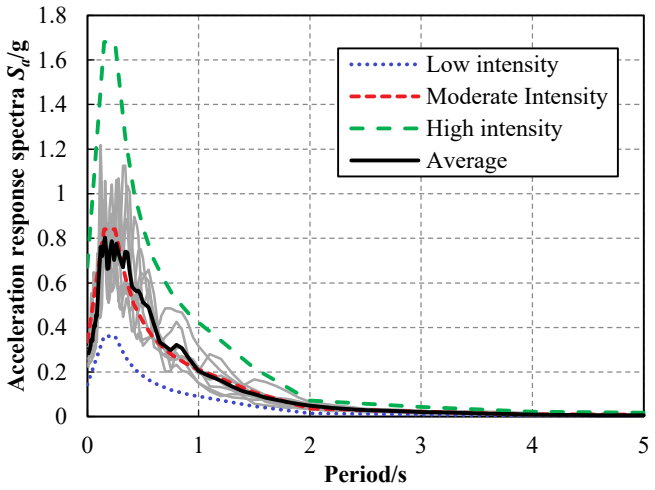

Fig. 11. The target spectra for the three intensities of earthquake motions in HK and the response spectra of the selected earthquake motion records

Table 3 Detailed information about the selected earthquake motion records

No.	Event	Year	Station	Magnitude	D_{cf}/km	V_{s30}/(m/s)	Orientation/°	$T_{5\text{-}95}$ (s)
1	Parkfield	1966	San Luis Obispo	6.19	63.34	493.5	234	17.8
2	San Fernando	1971	Castaic-Old Ridge Route	6.61	22.63	450.3	21	16.8
3	San Fernando	1971	Cedar Springs Pumphouse	6.61	92.59	477.2	126	10.2
4	San Fernando	1971	Upland-San Antonio Dam	6.61	61.73	487.2	15	14.3
5	Ierissos_Greece	1983	Ierissos	6.70	65.67	463.9	90	9.4
6	N. Palm Springs	1986	Whitewater Trout Farm	6.06	6.04	425.0	180	5.5
7	Loma Prieta	1989	WAHO	6.93	17.47	388.3	0	11.0

Note: D_{cf} is the distance to closest fault, $T_{5\text{-}95}$ is the duration of time over which is needed to build up between 5 and 95 percent of the total Arias intensity of a ground motion; and V_{s30} is the wave velocity of the upper 30m of the soil profile.

5.2. Feasibility assessment

5.2.1. Shear force

As shown in Fig. 12, the responses of shear force are enlarged in the close proportion to the PGAs corresponding to the three intensities, which indicates that the precast concrete shear wall can

maintain elastic even under the high intensity of earthquake motions. Shear force envelope rapidly reduces from the 1st story to about the 20th story, while it increases first and then decreases from about the 20th story to the 40th story. There is a peak value of shear force envelopes at about the 30th story. The peak value is not more than 30% of the maximum value of shear force envelope at the bottom, which reveals that shear failure most easily occurs at the bottom while other parts are relatively safe including the peak point.

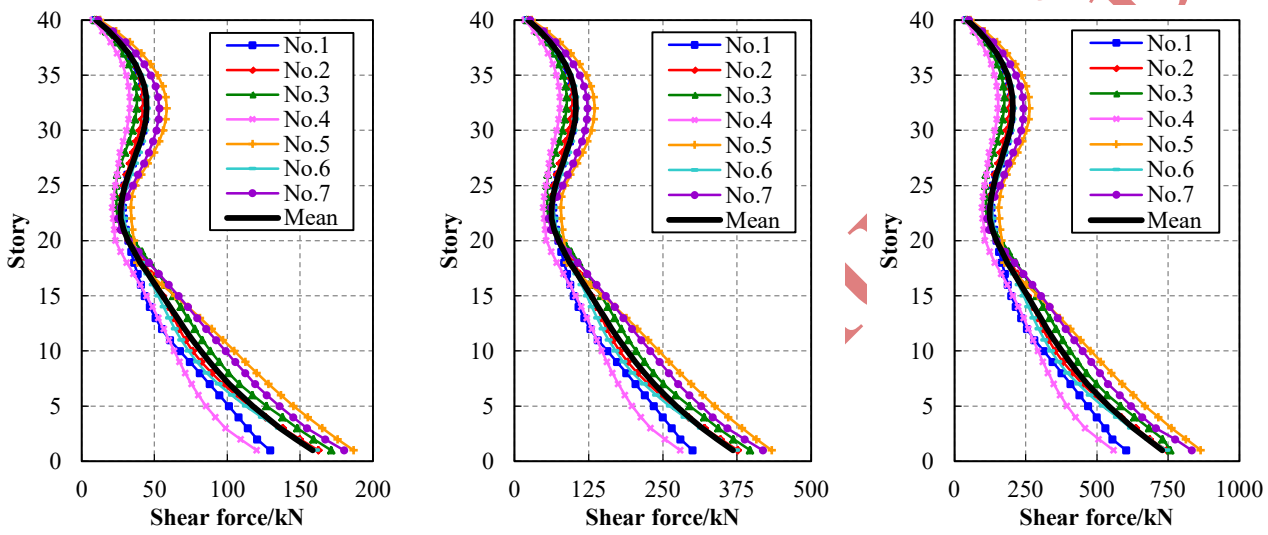

(a) Low intensity (b) Moderate intensity (c) High intensity

Fig. 12. Shear force envelopes of shear walls

Similarly, the capacity of resisting shear force at the bottom is calculated according to the concrete code of HK [41]. The time histories of demand-capacity ratio are calculated for the shear force at the bottom of the shear wall under the high intensity of earthquake motions. As shown in Fig. 13, the demand-capacity ratio of shear force is always not more than 0.2. The proposed lateral force resisting system is found to have enough capacity to resist the shear force caused by the high intensity of earthquake motions.

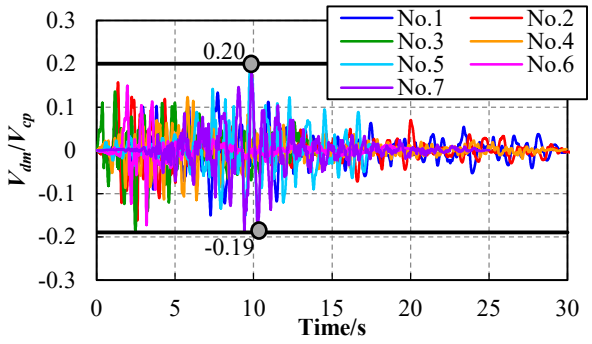

Fig. 13. The time histories of demand-capacity ratio for the shear force at the bottom of the shear wall under the high intensity of earthquake motions

5.2.2. Moment

The responses of moment are enlarged in a similar proportion to the PGAs corresponding to the different intensities (Fig. 14). Moment envelope is rapidly reduced from the 1st story to about the 10th story, while it is increased first and then decreased from about the 10th story to the 40th story. The peak value of moment envelope at about the 20th story is up to 66% of the moment at the bottom under the record No. 5, which indicates that the middle part of the shear wall is possible to become the second plastic hinge zone after plastic deformation occurs at the bottom.

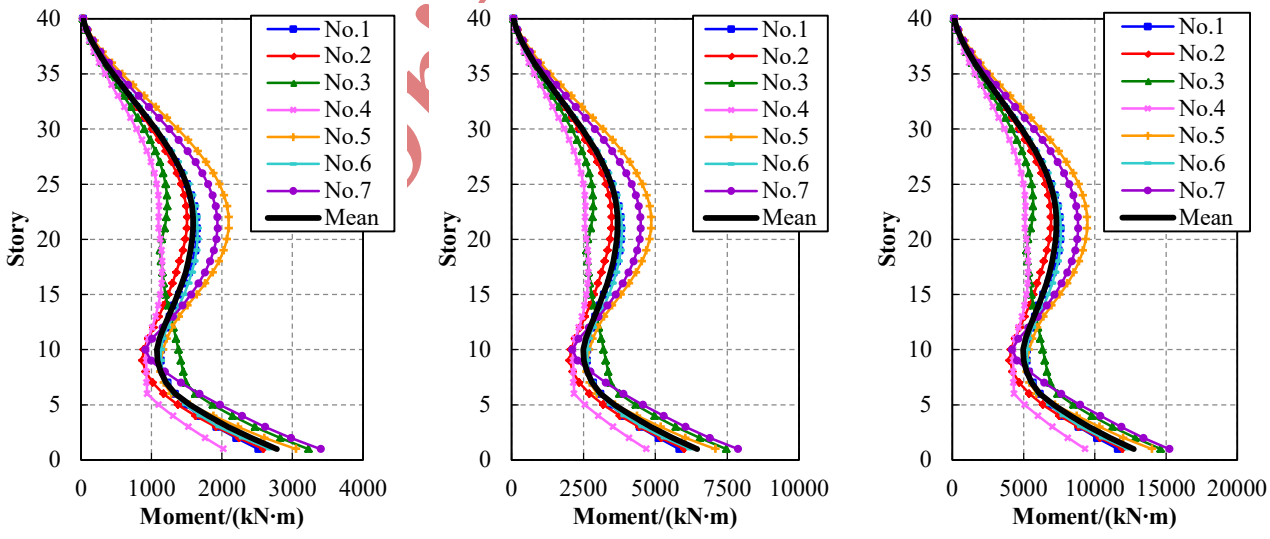

(a) Low intensity (b) Moderate intensity (c) High intensity

Fig. 14. Moment envelopes of shear walls

Similarly, the capacity of resisting moment at the bottom is obtained conducting sectional analysis. The time histories of demand-capacity ratio are calculated for the moment at the bottom of

the shear wall under the high intensity of earthquake motions. As shown in Fig. 15, the demand-capacity ratio of moment is always not more than 0.6. The proposed lateral force resisting system is found to have enough capacity to resist the moment caused by the high intensity of earthquake motions.

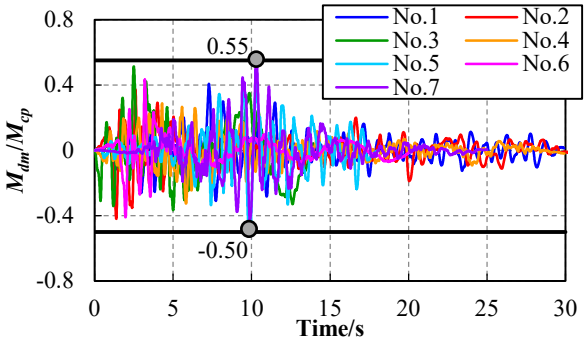

Fig. 15. The time histories of demand-capacity ratio for the moment at the bottom of the shear wall under the high intensity of earthquake motions

5.2.3. Deformation

As shown in Fig. 16, the responses of lateral deformation are enlarged in the identical proportion to the PGAs corresponding to the different intensities. Interstory drift ratio envelopes nonlinearly increase along the building height from the bottom to the top. The seismic code draft of HK [26] does not provide the limits of lateral deformation. Considering HK adjacent to Guangdong Province in China, the Chinese seismic code [43] can provide a reference. According to the Chinese code [43], the upper limits of interstory drift are 1/1000 (0.10%) at the low intensity level and 1/120 (0.83%) at the high intensity level, respectively. As shown in Fig. 16, the mean values of interstory drift envelope at the top are 0.049% at the low intensity level and 0.228% at the high intensity level, respectively. The proposed lateral force resisting system is found to have enough capacity to resist the lateral deformation caused by the different intensities of earthquake motions.

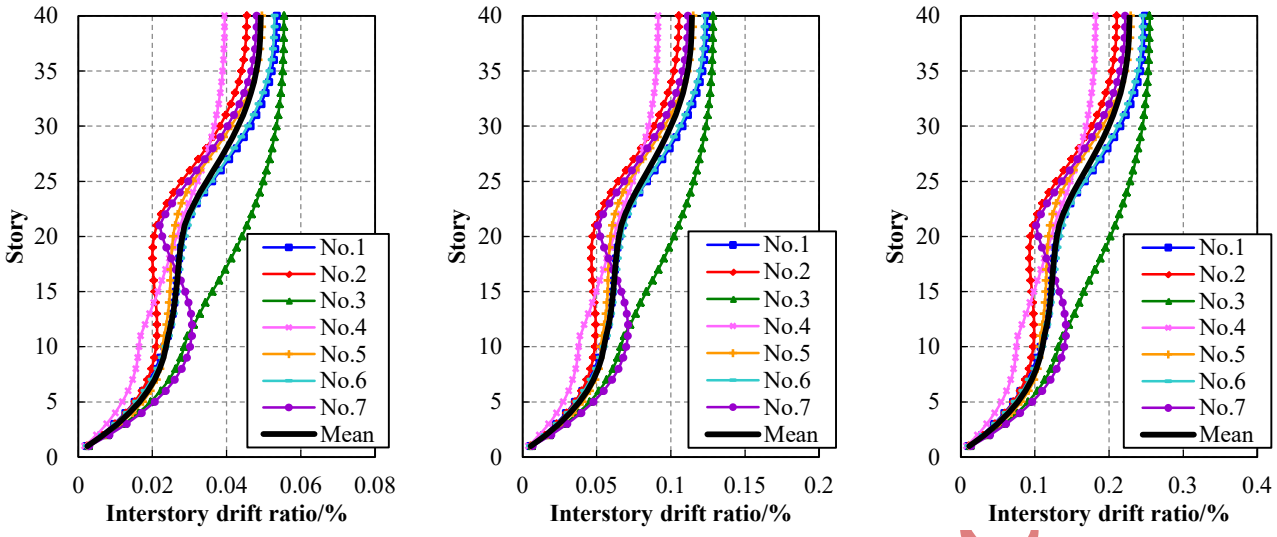

(a) Low intensity (b) Moderate intensity (c) High intensity

Fig. 16. Interstory drift envelopes of shear walls

6. Discussion on the effects of higher modes on seismic responses

6.1. Multi-modal analysis

Multi-modal analysis is carried out to study the effects of higher modes on seismic responses of the case building with the proposed lateral force resisting system. As shown in Fig. 17(a), different modal shapes and natural periods can be obtained using eigen-value analysis for a multi-freedom structure with known design parameters [44]. The modal shape vector can be normalized as

$$M_n = \{\phi_n\}^T [M] \{\phi_n\} = 1 \tag{6}$$

where M_n is the generalized modal mass of the n-th mode, $\{\phi_n\}$ is the normalized modal shape vector of the n-th mode, $[M]$ is the mass matrix.

$S_{a,n}$ is the spectral acceleration corresponding to the natural period T_n of the n-th mode when T_n is marked in the design acceleration spectrum (Fig. 17(b)). As shown in Fig. 17(c), each mode excites all the masses along the height according to its modal shape, and the seismic inertial force corresponding to the n-th mode can be determined as

$$\{v_n\} = \gamma_n S_{a,n} [M] \{\phi_n\} \tag{7}$$

where γ_n is the modal participation factors corresponding to the n-th mode and calculated as

$$\gamma_n = \{\phi_n\}^T [M]\{\iota\} / M_n \tag{8}$$

where $\{\iota\}$ is the static displacement vector of a structure caused by a unit ground displacement.

When the shear wall with the same mass m at each mass block is subject to the seismic inertial force $\{v_n\}$, the elastic shear force and moment at i mass block can be calculated as [45]

$$V_{ei,n} = \gamma_n S_{a,n} m \sum_{j=i}^{j=N} \phi_{j,n} \tag{9}$$

$$M_{ei,n} = \gamma_n S_{a,n} m \sum_{j=i}^{j=N} \phi_{j,n} \left(h_j - h_i\right) \tag{10}$$

where N is the total amount of mass blocks along the height. $V_{e0,n}$ and $M_{e0,n}$ are the elastic shear force and moment at the base caused by the seismic inertial force $\{v_n\}$, respectively. h_i is the height between i mass block and the base while h_j is the height between j mass block and the base.

Lateral deformation of the precast concrete shear wall is controlled by flexural behavior. The elastic curvature, rotation and lateral displacement at i mass block can be calculated only considering the flexural contribution as

$$\varphi_{ei,n} = \frac{M_{ei,n}}{EI_{eff}} \tag{11}$$

$$\theta_{ei,n} = \sum_{j=1}^{j=i} \varphi_{ej,n} \left(h_j - h_{j-1}\right) \tag{12}$$

$$\Delta_{ei,n} = \sum_{j=1}^{j=i} \theta_{ej,n} \left(h_j - h_{j-1}\right) \tag{13}$$

where EI_{eff} is the effective sectional stiffness and calculated as

$$EI_{eff} = \frac{M_y}{\varphi_y} \tag{14}$$

where M_y and ϕ_y are the yield moment and curvature of the shear wall, respectively. Considering the boundary conditions that the shear wall is fixed at the base, both the elastic rotation $\theta_{e0,n,}$ and lateral displacement $\Delta_{e0,n}$ at the base are equal to zero.

When $M_{ei,n}$ is more than M_y, the elastic moment $M_{ei,n}$ should be corrected to be the actual moment $M_{i,n}$ (Fig. 17(d)). When the sectional moment-curvature curve adopts the ideal elastoplastic model, the actual moment $M_{i,n}$ can be calculated as

$$M_{i,n} = \begin{cases} M_{ei,n} & M_{ei,n} \le M_y \\ M_y & M_{ei,n} > M_y \end{cases} \tag{15}$$

Similarly, the actual shear force $V_{i,n}$ can be calculated as

$$V_{i,n} = \begin{cases} V_{ei,n} & V_{ei,n} \le V_y \\ V_y & V_{ei,n} > V_y \end{cases} \tag{16}$$

The equal deformation principal is generally available for long-periodic structures [46]. The actual curvature $\varphi_{i,n}$ is equal to the elastic curvature $\varphi_{ei,n}$. Similarly, the actual rotation $\theta_{i,n}$ and lateral displacement $\Delta_{i,n}$ are equal to the elastic rotation $\theta_{ei,n}$ and lateral displacement $\Delta_{ei,n}$, respectively.

The contribution from each mode is combined using the square root of the sum of the squares (SRSS) procedure to obtain seismic demands including force and deformation as [46]

$$M_i = \sqrt{\sum_{n=1}^{N} M_{i,n}^2} \tag{17}$$

$$V_i = \sqrt{\sum_{n=1}^{N} V_{i,n}^2} \tag{18}$$

$$\Delta_i = \sqrt{\sum_{n=1}^{N} \Delta_{i,n}^2} \tag{19}$$

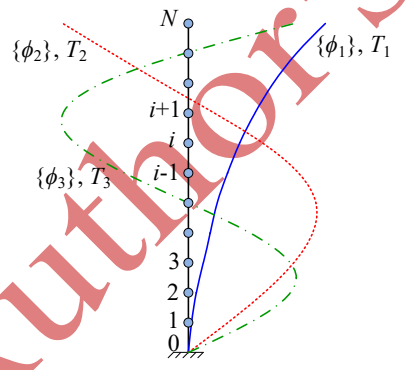

(a) Eigen-value analysis to give modal shapes and natural periods

N

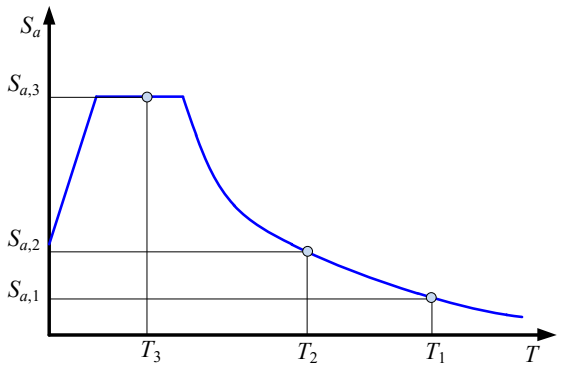

(b) Spectral accelerations corresponding to modal periods

M

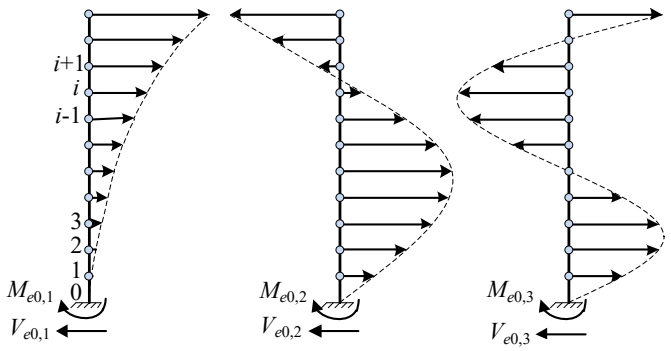

(c) Elastic responses caused by inertial forces of different modals

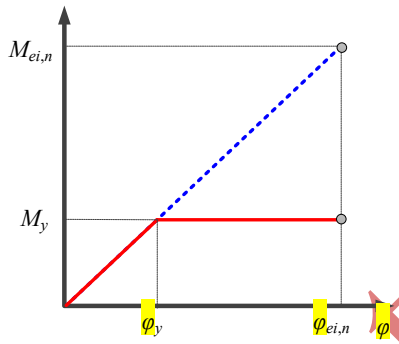

(d) Inelastic responses due to the principle of equal deformation

Fig. 17. Multi-modal analysis procedure

6.2. Comparison between multi-modal analysis and nonlinear dynamic analysis

The first ten natural periods and normalized modal shape vectors are obtained using the developed finite element for the precast concrete shear wall along the weak axis of the case building. The normalized modal shape vector $\{\phi_n\}$ has more half-waves along the height with n increased (Fig. 18).

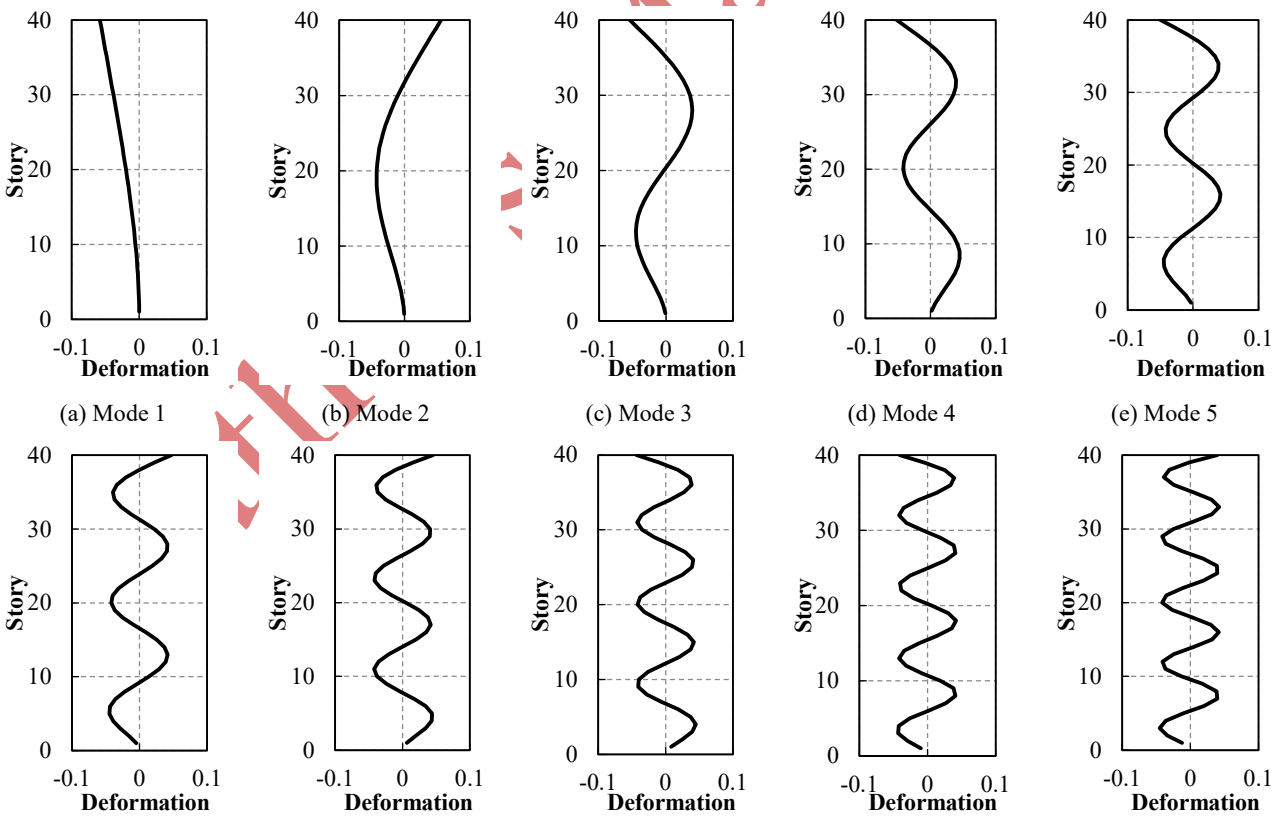

(a) Mode 1 (b) Mode 2 (c) Mode 3 (d) Mode 4 (e) Mode 5

(f) Mode 6 (g) Mode 7 (h) Mode 8 (i) Mode 9 (j) Mode 10

Fig. 18. The first ten normalized modal shape vectors of the shear wall along the weak axis of the case building

When the natural period T_n is known, $S_{a,n}$ can be determined according to the defined acceleration spectra of the design basis earthquake specified in the seismic design code draft of HK (Fig. 11). The modal participation factor γ_n can be calculated according to Eq. 8. Those results are listed in Table 4.

Table 4 Results of characteristic parameters corresponding to the first ten modes

Mode Type	1	2	3	4	5	6	7	8	9	10
T_n/s	5.705	0.910	0.325	0.166	0.100	0.067	0.048	0.036	0.028	0.022
$S_{a,n}$/g	0.007	0.231	0.656	0.840	0.672	0.571	0.504	0.470	0.437	0.403
γ_n	-26.39	-14.62	-8.57	6.13	-4.77	-3.90	3.30	2.86	-2.52	-2.26

The contribution from each mode is calculated and combined using the SRSS procedure to obtain seismic demands at each story of the precast concrete shear wall under the design basis earthquake motions (Fig. 19). SRSS-1, SRSS-2, and SRSS-3 represent the seismic demands by considering the contributions of the first one, two, and three modes, respectively.

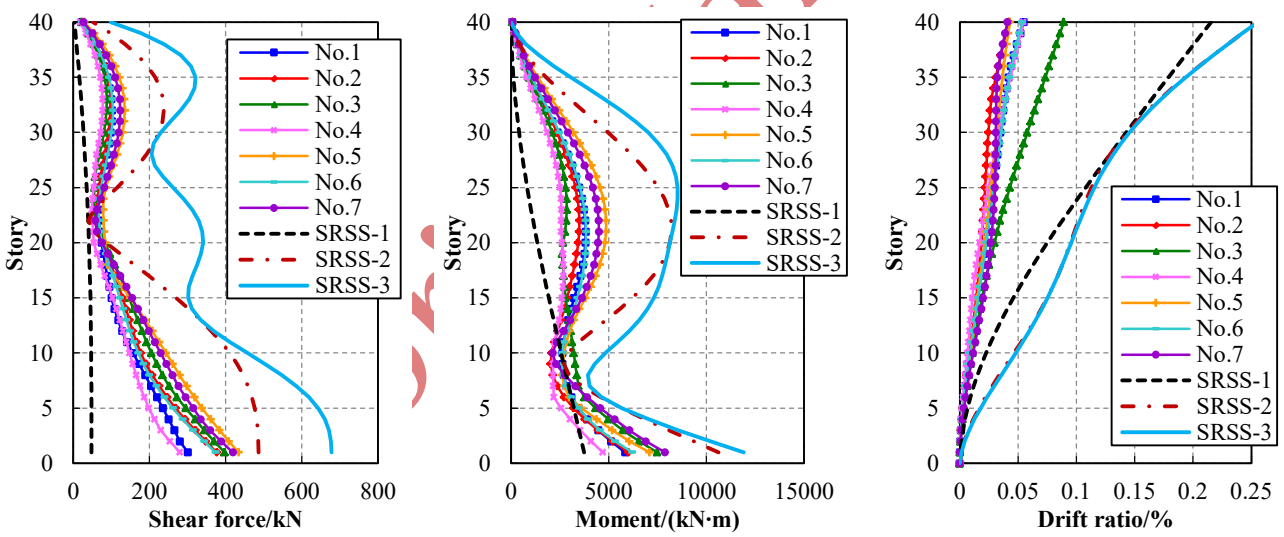

(a) Shear force (b) Moment (c) Lateral deformation

Fig. 19. Comparison between nonlinear dynamic analysis and multi-modes analysis for seismic demands of the precast concrete shear wall under the design basis earthquake motions

Compared with the seismic demand of shear force calculated by nonlinear dynamic analysis, SRSS-1 provides lower values in a quite another distribution pattern along the building height, SRSS-2 gives the closest envelope curve except for the inflection point in a comparable distribution pattern, and SRSS-3 presents conservative estimations in a more complex distribution pattern.

Meantime, compared with the seismic demand of moment by nonlinear dynamic analysis, SRSS-1 provides lower values except for the inflection point in a disparate distribution pattern, SRSS-2 gives the closest envelope curve in the basically same distribution pattern, and SRSS-3 presents a little more conservative estimations in a similar distribution pattern. Moreover, compared with the seismic demand of lateral deformation, SRSS-1 provides the closest envelope curve in a different distribution pattern, while both SRSS-2 and SRSS-3 give a little more conservative estimations in a closer distribution pattern. The above results indicate that higher modes have considerable effects on seismic demands including the absolute values at each story and the distribution pattern along the entire building height.

6.3. Contributions of higher-modes to seismic response

The following factors are defined to quantitatively measure the contribution of each mode to seismic demands at each story.

$$\xi_{n,M_i} = \frac{M_{i,n}^2}{\sum_{n=1}^{N} M_{i,n}^2} \tag{20}$$

$$\xi_{n,V_i} = \frac{V_{i,n}^2}{\sum_{n=1}^{N} V_{i,n}^2} \tag{21}$$

$$\xi_{n,\Delta_i} = \frac{\Delta_{i,n}^2}{\sum_{n=1}^{N} \Delta_{i,n}^2} \tag{22}$$

Although each mode has different contributions to different seismic demands at different stories, higher modes have significant even leading effects on seismic demands of shear force, moment, and lateral deformation at most stories (Fig. 20). The combination of the 2nd and 3rd modes provides the contribution of more than half to shear force along the entire building while the 1st mode basically has no effects. Meantime, the 2nd mode also plays a controlled role for the moment at most stories while the 1st mode has limited influence on the bottom of the shear wall. Moreover, the 1st mode dominates lateral deformation at the upper half of the shear wall while the 2nd mode does at the lower half.

Although the influence of each mode is relatively complex on seismic demands, a rule can still

be found that the cumulative proportion curve of seismic demands corresponding to the first *n* modes has *n* wave crests along the building height (Fig. 20). The shape of each mode seems to have a significant influence on its contribution distribution of seismic demands along the building height.

It is a meaningful issue that how to select modes to obtain the safe while not too conservative calculated results regarding the seismic demands of high-rise modular buildings with the proposed precast concrete shear walls. According to the results in Fig. 19, considering the first 3, 2, and 1 mode is capable to guarantee the calculated seismic demands of shear force, moment, and lateral deformation safe while not too conservative, respectively. As shown in Fig. 20, the cumulative proportions corresponding to the first 3, 2, and 1 mode are more than 50% on average along the entire building height for the seismic demands of shear force, moment, and lateral deformation, respectively. The calculated seismic demands may meet those requirements considering the contributions of the first *n* modes when the cumulative proportion corresponding to the first *n* modes is more than 50% on average along the entire building height. Nonetheless, the above proposed suggestion needs further verification.

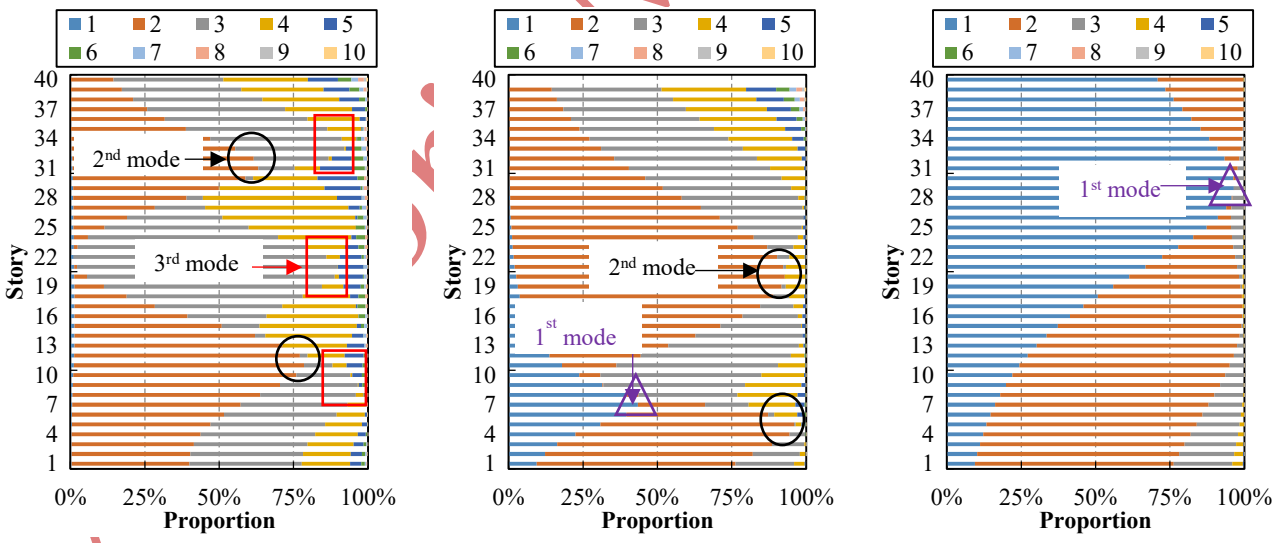

(a) Shear force (b) Moment (c) Lateral deformation

Fig. 20. Contributions of the first ten modes to seismic demands at each story

7. Conclusions

This paper has developed an innovative lateral force resisting system using precast concrete modules' walls as shear walls for high-rise buildings constructed using the modular approach. These

module walls replace traditional cast-in-situ cores or shear walls. A 40-story high-rise building based on public housing design in Hong Kong (HK) was adopted for case study. The structural performance of the precast concrete shear walls was simulated using a developed finite element (FE) model. The FE model considered the axial-flexure behavior of the precast concrete shear walls using the fiber section and its shear behavior with the definition of the uncoupled shear sectional property. The developed FE model was validated using the results of cyclic loading tests reported in the literature, and then was used to check the feasibility of the proposed lateral force resisting system for the case building under the wind and seismic loadings required in the relevant HK design codes. Multi-modal analysis was conducted to further study the effects of high-modes on seismic responses of the case building. The conclusions of the paper are listed below.

First, the developed FE model is verified to be effective to reproduce the structural performance of the precast concrete shear walls. There is an agreement between the calculated and experimental results of cyclic loading tests.

Second, the proposed lateral force resisting system is found to have enough strength and stiffness to resist the wind loading as specified in the wind code of HK. The demand-capacity ratios with 0.099 and 0.616 are less than 1.0 for the shear force and the moment at the bottom as the most vulnerable part. Meantime, the maximum drift ratio of 0.19% at the top is less than the upper limit of 0.20% as required in the HK code.

Third, the proposed lateral force resisting system is revealed to provide the capacity of resisting the seismic loading as required in the forthcoming HK seismic code. The proposed lateral force resisting system can remain elastic and has less lateral deformation than the corresponding code requirements when the case building is subject to the low, moderate, and high intensities of earthquake motions, respectively. Attributed to the effects of higher modes, the middle part of the precast concrete shear walls is possible to become the second plastic hinge zone after plastic deformation occurs at the bottom.

Fourth, higher modes have considerable even dominative effects on the seismic responses of the case building. A rule is found that the cumulative proportion curve of seismic demands

corresponding to the first n modes has n wave crests along the building height. The shape of each mode has a significant influence on its contribution distribution of seismic demands along the building height.

Finally, it is revealed to be applicable to use the cumulative contribution of modes to seismic demands to address how to select modes to calculate seismic demands of the high-rise modular buildings with the proposed system. According to this suggestion, the calculated seismic demands can balance safe and accuracy considering the contributions of the first n modes when the cumulative proportion of the first n modes is more than 50% on average along the entire building height. This suggestion shows a consensus with the results of nonlinear dynamic analysis, which may benefit from further verification.

This research focuses on the global lateral force resistance of high-rise modular buildings with the proposed lateral force resisting system under wind and seismic loadings. Future experimental research is recommended to further study the local robustness of connections in order to enable the rigid diaphragm. Also, the dynamic wind tunnel model studies should be conducted to consider the dynamic effect of wind loading on high-rise modular buildings using the proposed lateral force resisting system. Furthermore, it will be very meaningful to design and optimize the dimensions of modules for high-rise modular buildings considering the transportation, lifting, construction, and usage phases.

Acknowledgements

The work presented in this paper was supported by a grant from the Research Impact Fund of the Hong Kong Research Grants Council (Project No. R7027-18).

References

[1] Goodier CI, Pan W. The future of UK housebuilding. Royal Institution of Chartered Surveyors (RICS). London; 2010.

[2] Pan W, Gibb AG, Dainty AR. Leading UK housebuilders' utilization of offsite construction methods. Build Res Inf 2008; 36(1): 56-67.

[3] Pan W, Yang Y, Yang L. High-rise modular building: ten-year journey and future development. In Construction Research Congress, New Orleans, Apr. 2018; 523-532.

[4] Lacey AW, Chen W, Hao H, Bi K. Structural response of modular buildings-an overview. J Build Eng 2018; 16: 45-56.

[5] Liew JYR, Chua YS, Dai Z. Steel concrete composite systems for modular construction of high-rise buildings. Struct 2019; 21: 135-149.

[6] Lacey AW, Chen W, Hao H, Bi K. Review of bolted inter-module connections in modular steel buildings. J Build Eng 2019; 23: 207-219.

[7] Javed AA, Pan W, Chen L, Zhan W. A systemic exploration of drivers for and constraints on construction productivity enhancement. Built Environ Project Asset Manage 2018; 8(3): 239-252.

[8] Pan W, Su R, Cai Y, Young B. Engineering modular systems for high-rise buildings: an update. P I Civil Eng-Civ Eng 2018; 171(4): 148-148.

[9] Salimbahrami SR, Gholhaki M. Effects of higher modes and degrees of freedom (DOF) on strength reduction factor in reinforced concrete frames equipped with steel plate shear wall. Struct 2019; 19: 234-247.

[10] Annan CD, Youssef MA, El Naggar MH. Experimental evaluation of the seismic performance of modular steel-braced frames. Eng Struct 2009; 31(7): 1435-1446.

[11] Annan CD, Youssef MA, El Naggar MH. Seismic vulnerability assessment of modular steel buildings. J Earthq Eng 2009; 13(8): 1065-1088.

[12] Gunawardena T, Ngo TD, Mendis P, Aye L, Alfano J. Structural performance under lateral loads of innovative prefabricated modular structures. In: B. Samali, M.M. Song, C. Attard (Eds.), From Materials to Structures: Advancement Through Innovation, London: Taylor & Francis; 2013.

[13] Gunawardena T, Ngo T, Mendis P. Behaviour of multi-storey prefabricated modular buildings under seismic loads. Earthq Struct 2016; 11(6): 1061-1076.

[14] Gunawardena T, Ngo T, Mendis P, Alfano J. Innovative flexible structural system using prefabricated modules. J Archit Eng 2016; 22(4): 05016003.

[15] Styles AJ, Luo FJ, Bai Y, Murray-Parkes JB. Effect of joint rotational stiffness on structural responses of multi-story modular buildings. In: Proc. the International Conference on Smart Infrastructure and Construction, London: ICE Publishing, Jun. 2016.

[16] Fathieh A, Mercan Q. Seismic evaluation of modular steel buildings. Eng Struct 2016; 122: 83-92.

[17] Srisangeerthanan S, Hashemi MJ, Rajeev P, Gad E, Fernando S. Numerical study on the effects of diaphragm stiffness and strength on the seismic response of multi-story modular buildings. Eng Struct 2018; 163: 25-37.

[18] Shan S, Looi D, Cai Y, Ma P, Chen MT, Su R, Young B, Pan W. Engineering modular integrated construction for high-rise building: a case study in Hong Kong. P I Civil Eng-Civ Eng 2019; 1-7.
[19] Pan W, Pan M. A dialectical system framework of zero carbon emission building policy for high-rise high-density cities: Perspectives from Hong Kong. J Clean Prod 2018; 205: 1-13.
[20] Pan W, Hon CK. Modular integrated construction for high-rise buildings. P I Civil Eng-Munic Eng 2018; 1-12.
[21] Lawson RM, Ogden RG, Bergin R. Application of modular construction in high-rise buildings. J Archit Eng 2011; 18(2): 148-154.
[22] Xu G, Wang Z, Wu B, Bursi OS, Tan X, Yang Q, Wen L, Jiang H. Pseudodynamic tests with substructuring of a full-scale precast box-modularized structure made of reinforced concrete shear walls. Struct Des Tall Spec 2017; 26(16): e1354.
[23] Zheng Y, Guo Z, Guan D, Zhang X. Parametric study on a novel grouted rolling pipe splice for precast concrete construction. Constr Build Mater 2018; 166: 452-463.
[24] Xu G, Wang Z, Wu B, Bursi OS, Tan X, Yang Q, Wen L. Seismic performance of precast shear wall with sleeves connection based on experimental and numerical studies. Eng Struct 2017; 150 346-358.
[25] Buildings Department. Code of practice for dead and imposed loads, Hong Kong; 2011.
[26] Buildings Department. Consultancy study on seismic-resistant design standards for buildings in Hong Kong (Consultancy agreement No. 9OC101), Hong Kong; 2017.
[27] Ji X, Liu D, Sun Y, Molina HC. Seismic performance assessment of a hybrid coupled wall system with replaceable steel coupling beams versus traditional RC coupling beams. Earthq Eng Struct Dyn 2017; 46(4): 517-535.
[28] Tang Y, Zhang J. Probabilistic seismic demand analysis of a slender RC shear wall considering soil-structure interaction effects. Eng Struct 2011; 33(1): 218-229.
[29] Orakcal K, Wallace JW. Flexural modeling of reinforced concrete walls-experimental verification. ACI Mater J 2006; 103(2): 196-206.
[30] Lu X, Xie L, Guan H, Huang Y, Lu X. A shear wall element for nonlinear seismic analysis of super-tall buildings using OpenSees. Finite Elem Anal Des 2015; 98: 14-25.
[31] Sun J, Qiu H, Lu Y. Experimental study and associated numerical simulation of horizontally connected precast shear wall assembly. Struct Des Tall Spec 2016; 25(13): 659-678.
[32] Wallace JW. Modelling issues for tall reinforced concrete core wall buildings. Struct Des Tall Spec 2007; 16(5): 615-632.
[33] Martinelli P, Filip FC. Simulation of the shaking table test of a seven-story shear wall building. Earthq Eng Struct Dyn 2009; 38(5): 587-607.
[34] Luu H, Ghorbanirenani I, Léger P, Tremblay R. Numerical modeling of slender reinforced concrete shear wall shaking table tests under high-frequency ground motions. J Earthq Eng 2013; 17(4): 517-542.
[35] Mazzoni S, McKenna F, Scott MH, Fenves GL. OpenSees command language manual. Pacific Earthquake Engineering Research Center (PEER), Berkeley; 2006.
[36] Kent DC, Park R. Flexural members with confined concrete. J Struct Div 1971; 97(7): 1969-1990.
[37] Rahal KN. Post-cracking shear modulus of reinforced concrete membrane elements. Eng Struct 2010; 32(1): 218-225.
[38] Thomsen IV, John H, Wallace JW. Displacement-based design of slender reinforced concrete structural

walls-experimental verification. J Struct Eng 2004; 130(4): 618-630.
[39] Birely A, Lehman D, Lowes L, Kuchma D, Hart C, Marley K. Investigation of the seismic behavior and analysis of reinforced concrete structural walls. In: Proc. 14th World Conference on Earthquake Engineering, Beijing, Aug. 2008.
[40] Buildings Department. Code of practice on wind effects in Hong Kong. Hong Kong; 2004.
[41] Buildings Department. Code of practice for structural use of concrete. Hong Kong; 2013.
[42] Buildings Department. Consultation paper for introducing seismic-resistant building design standards in Hong Kong. Hong Kong; 2011.
[43] JGJ 3-2010. Technical specification for concrete structures of tall building. China Ministry of Construction, Beijing, 2010. (in Chinese).
[44] Sullivan TJ, Priestley MJN, Calvi GM. Estimating the higher-mode response of ductile structures. J Earthq Eng 2008; 12(3): 456-472.
[45] Chen X, Guan Z, Spencer JBF, Li J. A simplified procedure for estimating nonlinear seismic demand of tall piers. Eng Struct 2018; 174: 778-791.
[46] Miranda E, Bertero VV. Evaluation of strength reduction factors for earthquake-resistant design. Earthq Spectra 1994; 10(2): 357-379.